Received: 02 October 2020 | Revised: 09 December 2020 | Accepted: 14 December 2020
DOI: 10.22034/ecc.2020.250966.1079
Eurasian Chemical Communications
SAMI

FULL PAPER

Single crystal X-Ray structure and DFT-D3 studies on 2-amino-4-(2,4-dichlorophenyl)-6-phenylnicotinonitrile

Zahra Hosseinzadeh[a,*] |Mohammad Khavani[b] |Ali Ramazani[a,c,*] |Hamideh Ahankar[d] |Vasyl Kinzhybalo[e]

[a]*Department of Chemistry, University of Zanjan, P.O. BOX 4537138791, Zanjan, Iran*

[b]*Department of Chemistry and Materials Science, School of Chemical Engineering, Aalto University, P.O. BOX 16100, FI-00076 Aalto, Finland*

[c]*Research Institute of Modern Biological Techniques, University of Zanjan, P.O. BOX 4537138791, Zanjan, Iran*

[d]*Department of Chemistry, Abhar Branch, Islamic Azad University, P.O. BOX 22, Abhar, Iran*

[e]*Institute of Low Temperature and Structure Research, PAS, 2 Okólna St., 50-422 Wrocław, Poland*

***Corresponding Authors:**
Zahra Hosseinzadeh & Ali Ramazani
Email: zahra.hosseinzadeh@znu.ac.ir & aliramazani@gmail.com
Tel.: +024 33052572

The crystal structure of 2-amino-4-(2,4-dichlorophenyl)-6 phenylnicotinonitrile (ADPN) was determined by single crystal X-ray diffraction. The crystal structure showed two independent molecules with very similar geometric parameters and different environments. Density functional theory (DFT) and DFT dispersion corrected (DFT-D3) calculations were applied to study the structural and chemical properties of ADPN and its dimer. To have a better insight into the properties of the synthesized molecule, quantum chemistry calculations were performed. Based on the calculated results, the dispersion forces have remarkable effects on the stability of ADPN crystal. Moreover, hydrogen bond interactions between ADPN molecules due to molecular orbital interactions can be a driving force for the dimerization process.

KEYWORDS

2-Amino-4-(2,4-dichlorophenyl) -6-phenylnicotinonitrile; single crystal x-ray structure; DFT-D3; hydrogen bond; quantum chemistry calculation.

Introduction

Many attempts have been made to develop novel efficient and green synthetic methods for the preparation of heterocyclic compounds because of their high importance in the medicinal science. Heterocyclic compounds with the pyridine scaffold demonstrated a wide variety of biological effects such as antimicrobial, antihypertensive, A2A adenosine receptor antagonizing, cardiovascular, antipyretic, strong inhibitor of HIV-1 integrase, anti-inflammatory, and anti-parkinsonism properties. These multiple pharmaceutical effects have made them interesting synthetic targets. They are also selective inhibitors of IKK-β serine-threonine protein kinase. In fact, these outstanding pharmacophore skeletons are well-known for their biological effects [1-3]. An integral part of numerous natural products such as coenzyme vitamin B_6 family and many alkaloids have been formed from the pyridine scaffold [4,5].

In the past decades, multicomponent reactions (MCRs) based on the synthesis of widespread and diverse heterocyclic compounds have been noticed in organic synthesis by chemists and scientists [6-9]. There are several works in the literature concerning the synthesis of 2-amino-4,6-diarylnicotinonitrile derivatives by MCRs [10-13]. We have also synthesized 2-amino-4,6-diarylnicotinonitriles in the presence of acidic

catalysts [14, 15]. We have reported the good cytotoxic activity and the potentiality to bind to the Eg5 binding site (as a validated molecular target) of 2-amino-4-(2,4-dichlorophenyl)-6-phenylnicotinonitrile ADPN) [15]. In the context of our general interest in the synthesis of heterocycle compounds, using single crystal X-ray structure, and DFT studies [16-18], we report the characterization and crystal structure of continuation of ADPN. To have a better insight into the properties of the synthesized molecule, we performed quantum chemistry calculations. As shown in Figure 1, this derivative has been synthesized from the reaction of 2,4-dichlorobenzaldehyde, acetophenone, malononitrile, and ammonium acetate in the presence of boric acid as a green catalyst under microwave irradiation [14]. The structure of the title product 2-amino-4-(2,4-dichlorobenza dichlorophenyl)-6-phenylnicotinonitrile (ADPN) was determined by FT-IR, ^{1}H NMR, and ^{13}C NMR spectroscopic data [14] (See Figures S1 to S3 in Supplementary Information respectively). Moreover, single crystal X-ray analysis was performed in this work.

Preparation of crystals

After recrystallization of the target product from hot ethanol, the pure powder of 2-amino-4-(2,4-dichlorophenyl)-6-phenylnicotinonitrile (ADPN) was dissolved in hot ethanol. X-ray quality crystals were obtained in excellent yield after slow evaporation of the mother liquor at room temperature.

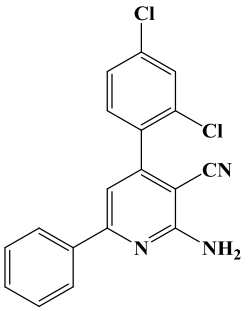

FIGURE 1 Structure of 2-amino-4-(2,4-dichlorophenyl)-6-phenylnicotinonitrile

Results and discussion

Density functional theory (DFT) and DFT dispersion corrected (DFT-D3) calculations were used to study the structural and chemical properties of ADPN and its dimer. The structures of ADPN and ADPN dimer were optimized by using BP86 and BP86-D3 functionals with 6-31+G(d) basis set [19, 20]. In order to calculate the thermodynamic parameters during dimerization process frequency calculations were applied. The BP86-D3 functional in contrast to BP86 can describe dispersion interactions; therefore, by employing these functionals, dispersion interactions were calculated.

To investigate the charge transfer and electrostatic interactions inside the ADPN dimer, natural bond orbital (NBO) analysis was performed [21]. By employing NBO analysis, we can study the molecular orbital and donor-acceptor interactions in ADPN dimer. Gaussian 09 computational package was applied for these quantum chemistry calculations [22].

Finally, to determine the nature of interactions between ADPN in dimer structure quantum theory of atoms in molecules (QTAIM) [23], 2D- and 3D-non covalent interaction (NCI) [24] analyses were applied by using MultiWFN 3.4 [25].

X-Ray crystallography

The structure determination of ADPN was carried out on an Oxford Diffraction Xcalibur κ-geometry four-circle diffractometer equipped with an Atlas CCD detector and graphite-monochromated Mo Kα radiation (λ=0.71073 Å). The data collection was carried out at 100(2) K with the use of the *Oxford-Cryosystems 800* series cryocooler. Diffraction data were corrected for the polarization and Lorentz effects. Data collection, cell refinement, along with data reduction and analysis were carried out with the CrysAlisPro program package [26]. Analytical shape-based absorption correction was introduced. The

crystal structure was solved using SHELXT-2014 [27] and refined by a full-matrix least squares method with the anisotropic thermal parameters for all non-H atoms with the use of SHELXL-2014 [28]. Hydrogen atoms were located in different Fourier maps. In the final refinement cycles, C/N-bound H atoms were put in their calculated positions and refined with a riding model, so that C–H=0.95 Å, N–H=0.88 Å and with U_{iso}(H)=1.2U_{eq}(C/N). One of two independent molecules is slightly orientationally disordered, 2,4-dichlorophenyl substituent was split into two positions with the geometry of minor part restricted to be the same as the major. Figures were prepared using the DIAMOND program [29]. The crystallographic information file (CIF) was deposited with The Cambridge Crystallographic Data Centre (http://www.ccdc.cam.ac.uk/; deposition number CCDC 1882629 and published as ESI.

Crystal data for ADPN. $C_{18}H_{11}Cl_2N_3$, M_r=340.20, colorless block, crystal dimensions 0.50 × 0.38 × 0.34 mm, monoclinic, sp. gr. $P2_1/c$, a=9.421(3), b=27.617(6), c=12.501(4) Å, β=106.31(3)°, V=3121.6(16) Å^3, T=100(2) K, Z=8, μ=0.42 mm^{-1} (for Mo Kα, λ=0.71073 Å), analytical shape-based absorption correction, T_{min}=0.89, T_{max}=0.91, 34539 measured reflections, 7849 unique (R_{int} =0.028), 6415 observed (I >2σ(I)), (sin θ/λ)$_{max}$ = 0.696 Å^{-1}, 448 parameters, 28 restraints, R=0.036, wR = 0.091 (observed refl.), GOOF=S=1.03, ($\Delta\rho_{max}$) = 0.35 and ($\Delta\rho_{min}$)=−0.27 e Å^{-3}.

The molecular structure of the title compound was confirmed by single-crystal X-ray crystallography. The independent part of the structure and the numbering scheme are shown in Figure 2. It consists of two independent molecules referred to as A and B. Molecule A is slightly disordered over two positions with 2,4-dichlorophenyl ring atoms' occupancies equal to 96.63(12)% and 3.37(12)%, respectively. The geometric parameters of the molecules A and B are quite similar, seeming to be related by a non-crystallographic pseudoinversion center at around (0.49, 0.37, 0.47). The root mean-square distance between respective atoms of overlaid A and inverted B molecules is equal to 0.071 Å (a minor part of the disorder is neglected). The molecule of the title compound consists of three rings: central pyridyl ring, phenyl, and 2,4-dichlorophenyl rings. Average planes fitted to the rings form the following dihedral angles in A and B molecules: 13.35(7)° and 13.48(7)° for ∠(N1/C5, C6/C11), 57.59(9)° and 54.32(7)° for ∠(N1/C5, C13/C18).

Main intermolecular interaction is observed between independent A and B molecules leading to the formation of the dimer by a pair of hydrogen bonds between the amino group hydrogen atom and the nitrogen atom of the nitrile (Figure 3), with the following geometrical parameters: N2A–H2AB···N3B, D–H 0.88 Å, H···A 2.26 Å, D···A 3.0685(19) Å, ∠(D–H···A) 152.2° and N2B–H2BB···N3A D–H 0.88 Å, H···A 2.20 Å, D···A 3.0117(19) Å, ∠(D–H···A) 153.4°. There are no other strong or intermediate hydrogen bonds in the crystal structure. Above mentioned dimers are further connected by stacking π-π interactions into tetramers: C13B/C18B···(C13B/C18B)^i Cg···Cg^i 3.81 Å, interplanar distance 3.45 Å, offset 1.62 Å (symmetry code: (i) 1-x, 1-y, 2-z). These tetramers are connected into chains (Figure 3) in an axis direction through Cl···Cl interactions between symmetry related Cl2B atoms: Cl2B···Cl2B^{ii} 3.131 Å (symmetry code: (ii) -x, 1-y, 2-z).

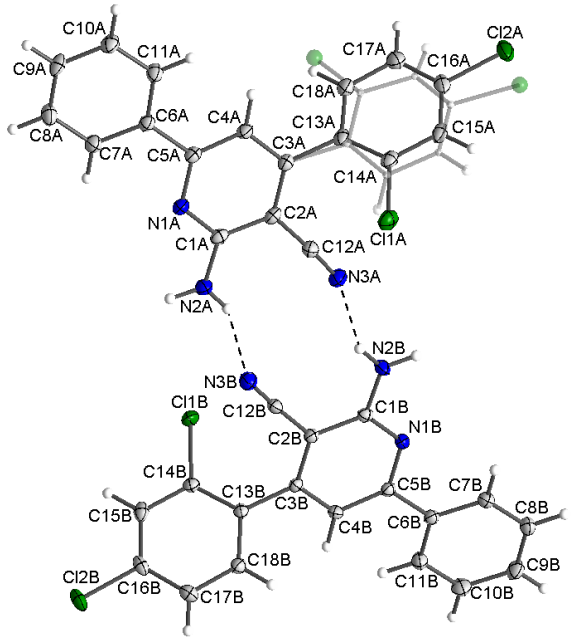

FIGURE 2 Asymmetric part of the structure of 2-amino-4-(2,4-dichlorophenyl)-6-phenylnicotinonitrile along with the numbering scheme. The Minor part of the disordered 2,4-dichlorophenyl ring is shown by transparent lines. Atomic displacement ellipsoids are shown at the 50% probability level

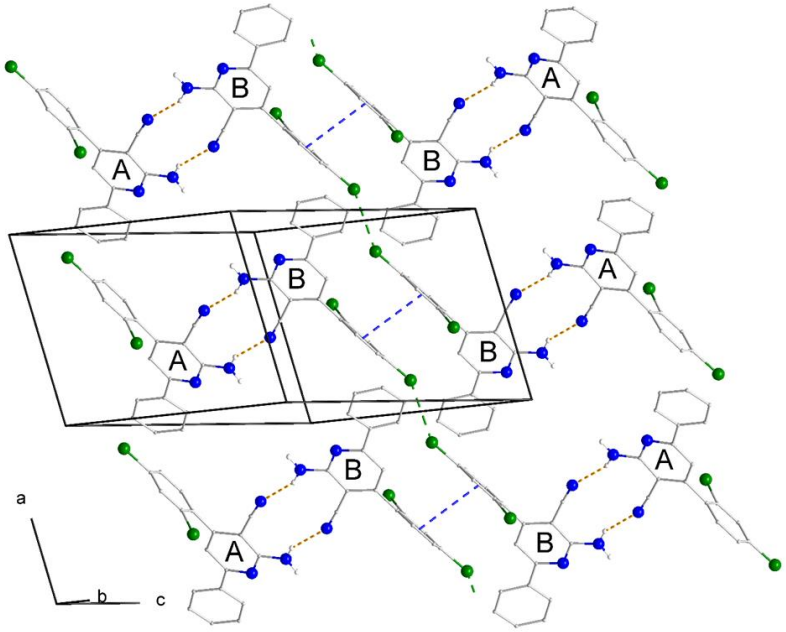

FIGURE 3 Crystal packing of the ADPN structure. The minor part of the disordered 2,4-dichlorophenyl ring and C-bound hydrogen atoms are omitted for clarity. Hydrogen bonds, π-π, Cl···Cl interactions are shown with orange, blue, and green broken lines, respectively

Structural analysis

Figure 4 shows the optimized structures of ADPN and ADPN dimer in the gas phase. According to Table 1, the calculated structural parameters are in good agreement with crystallographic data. For example, the

calculated bond lengths for C15–Cl16, C15–C17, C13–H14, C9–C10, and C2–N3 are 1.75, 1.40, 1.09, 1.49 and 1.37 Å and the experimental bond length for the corresponding bonds are 1.73, 1.38, 0.97, 1.48 and 1.35 Å, respectively. Moreover, the calculated H14–C13–C15 and C11–C13–C15 angles by theoretical methods confirmed the experimental values. The calculated values for these angles are 117.75 and 118.79°, which are in good agreement with the experimental results.

Moreover, the structural analysis confirmed the hydrogen bond (H-bond) formation between ADPN in the dimer structure. The calculated N–H bond length of the ADPN monomer is 0.98 Å, which due to dimerization increases to 1.03 Å, confirming a remarkable interaction or H-bond formation between ADPN monomers. To analyze the conformation properties of ADPN dihedral scan calculation for C6/C9/C10/C11 angle was applied. According to the obtained results, there are three structural conformers for ADPN, as shown in Figure S4 in Supplementary Information. Based on the calculated energies, the conformer 2 (Figure S4) has the most stable structure, which is consistent with the crystallographic data. Moreover, NMR calculations were employed at the BP86/6-13G(d) level of theory. The calculated NMR spectra (see supporting information) clearly show the difference in geometrical properties for the ADPN.

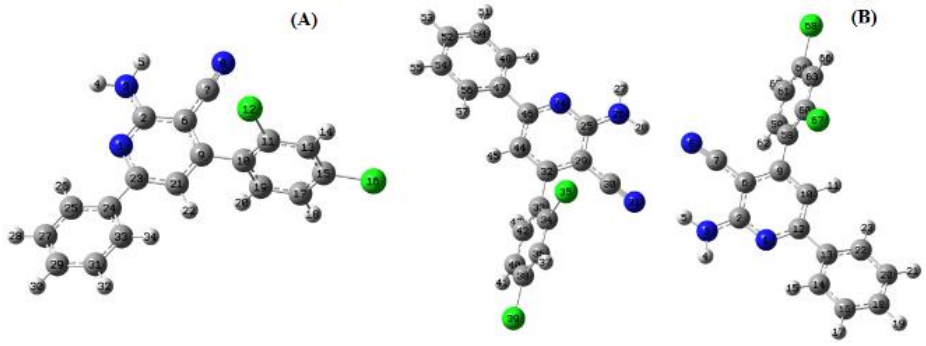

FIGURE 4 The optimized structures of ADPN monomer (A) and its dimer (B) with atom numbering at BP86/6-31+G(d) level of theory

TABLE 1 The calculated geometrical parameters of ADPN and its dimer at BP86/6-31+G(d) level of theory (bonds and angles are in Å and degree, respectively)

Monomer			Dimer		
Parameters	**Theory**	**Experimental**	**Parameters**	**Theory**	**Experimental**
C15–Cl16	1.75	1.73	H28···N8	2.02	2.19
C17–C15	1.40	1.38	N31···H5	2.02	2.26
C13–H14	1.09	0.97	C8–N7	1.17	1.14
C9–C10	1.49	1.48	N3–H5	1.02	0.93
C7–N8	1.18	1.15	C2–C6	1.44	1.42
C2–N3	1.37	1.35	C7–N8···H28	161.70	157.90
Cl12–C11–C13	117.75	117.04	C6–C2–C29	79.34	81.50
H14–C13–C15	120.88	120.72	C7–C6–C2	119.73	118.06
C11–C13–C15	118.79	118.59	C26–C25–C29	122.03	121.82
C9–C10–C11	123.02	124.50	H28–H5–N3	146.20	157.86
C6–C9–C10–C11	73.40	57.68	C29–C30–C7–C6	174.72	171.85

Table 2 shows the thermodynamic parameters of the ADPN dimerization process. Calculated values of binding energy (ΔE), enthalpy energy (ΔH), and Gibbs energy (ΔG) by BP86-D3 functional are greater than those from BP86 functional, which confirms an important contribution of dispersion forces. According to Table 2, the negative values of ΔE show the considerable stability of ADPN dimer and the negative values of ΔH reveal that the dimerization process is exothermic. Moreover, the calculated values of ΔG by different functionals confirmed that the dimerization process is favorable from the thermodynamic point of view.

TABLE 2 The calculated thermodynamic parameters (kcal·mol^{-1}) of the ADPN dimerization process by different functionals

	ΔE	**ΔH**	**ΔG**
BP86	-7.53	-8.13	-1.77
BP86-D3	-15.56	-16.15	-3.36
	ΔE_{dis}	ΔH_{dis}	ΔG_{dis}
(BP86-D3)-BP86	-8.03	-8.02	-1.59

The calculated dispersion binding energy (ΔE_{dis}) for the dimerization process is -8.03 kcal·mol^{-1}. According to the structural analysis, each dimer can form two N–H···N bonds, so the H-bond interaction energy for each bond is -4.01 kcal·mol^{-1}. These results are in good agreement with the reported values in the literature [30]. It is well worth mentioning that the negative values of the calculated dispersion thermodynamic parameters reveal that dispersion forces have a considerable role in the crystal stability of ADPN.

Quantum reactivity indices and molecular orbital interaction

To investigate the electrostatic and donor–acceptor interactions between ADPN in dimer structure, we did NBO analysis. By employing this method, stabilization energy values, E(2), were calculated. Using the NBO method, it is possible to find related information about the interactions of orbitals. Second-order perturbation theory analysis was employed to calculate the donor–acceptor interactions. In this analysis, the stabilization energy, E(2), is related to the molecular orbital interactions; when the E(2) energy between a donor and an acceptor group is large, there is a strong interaction. For each donor orbital (i) and acceptor orbital (j), E(2) is associated with i → j delocalization and is given by equation 1:

$$E(2)= \Delta E_{i,j}= q_i \{F^2 (i,j) / (E_j - E_i)\} \quad (1)$$

where q_i is the *i*th donor orbital occupancy, E_i and E_j are diagonal elements, and (i,j) are off-diagonal elements of the Fock matrix.

Table 3 shows the most important donor-acceptor interactions between lone pair (Lp) electrons of N atoms and bonding orbitals (σ and π) as a donor with antibonding orbitals (σ* and π*) of different bonds as an acceptor. The calculated E(2) values for the ADPN monomer shows strong orbital interactions between bonding orbitals of N1–C2 bond (π_{N1C2}) with antibonding orbital of C21–C23 bond (π^*_{C21C23}). In dimer structure, there are considerable orbital interactions for $\pi_{C2C6} \rightarrow \pi^*_{C7N8}$, $\pi_{C2C6} \rightarrow \pi^*_{C9C10}$, $\pi_{N1C12} \rightarrow \pi^*_{C2C6}$. The calculated E(2) values for the interaction between LP electrons of N8 and N31 atoms with an antibonding orbital of N26–H28 and N3–H5 bond, respectively, confirming H-bond formation between ADPN monomers. In other words, the origin of the dimer stability is H–bond formation because of strong molecular orbital interactions between (Lp) electrons of N atoms and σ^*_{NH} orbitals.

To investigate the reactivity of ADPN and its dimer, the HOMO-LUMO analysis was applied. Based on the HOMO and LUMO, we can describe the reactivity of a molecule. E_H and E_L are HOMO and LUMO energies, respectively. The lower value of E_{LUMO},

indicates that the molecule would accept electrons. Figure 5 shows the HOMO and LUMO diagrams of ADPN and its dimer. According to Figure 5, the HOMOs locate on heteroatoms of ADPN, while LUMOs show a contrast pattern. In other words, LUMOs extend to the whole molecule in comparison to HOMOs, especially for the dimer structure.

TABLE 3 The calculated E(2) values (kcal·mol^{-1}) for different donor- acceptor interactions at **BP86/6-31+G(d) level of theory**

Monomer		Dimer	
Donor →Acceptor	E(2)	Donor →Acceptor	E(2)
$\pi_{C2N3} \rightarrow \pi^*_{N1C23}$	2.18	$\sigma_{C2N3} \rightarrow \pi^*_{N1C12}$	2.12
$\pi_{C2C6} \rightarrow \pi^*_{N3H4}$	1.94	$\pi_{C2C6} \rightarrow \pi^*_{C7N8}$	21.44
$\sigma_{N3H4} \rightarrow \pi^*_{C2C6}$	4.53	$\pi_{C2C6} \rightarrow \pi^*_{C9C10}$	20.17
$\pi_{C6C7} \rightarrow \pi^*_{C7N8}$	3.66	$\sigma_{N3H5} \rightarrow \pi^*_{N1C2}$	4.25
$\pi_{N1C2} \rightarrow \pi^*_{C21C23}$	21.91	$\pi_{N1C12} \rightarrow \pi^*_{C2C6}$	23.76
$\pi_{N1C23} \rightarrow \pi^*_{C2N3}$	3.53	$\pi_{N1C126} \rightarrow \pi^*_{C9C10}$	7.09
$\pi_{C6C9} \rightarrow \pi^*_{C2N3}$	3.08	$\pi_{N1C12} \rightarrow \pi^*_{C13C22}$	7.22
$\pi_{C6C9} \rightarrow \pi^*_{C2C6}$	3.08	$\pi_{C9C10} \rightarrow \pi^*_{N1C12}$	21.70
$Lp_{N1} \rightarrow \sigma^*_{C2N3}$	3.08	$\pi_{C9C10} \rightarrow \pi^*_{C2C6}$	9.57
$Lp_{N1} \rightarrow \pi^*_{C2C6}$	10.43	$Lp_{N8} \rightarrow \pi^*_{N26H28}$	11.93
$Lp_{N1} \rightarrow \pi^*_{C21C23}$	8.96	$Lp_{N31} \rightarrow \pi^*_{N3H5}$	12.04

According to Table 4, due to dimerization E_L and E_H values decrease and dimer structure has a lower band gap (ΔE_{L-H}) in comparison to the ADPN monomer. This result indicates that the dimerization increases the reactivity of the ADPN molecule. Moreover, the calculated chemical potential (μ) reveals that dimerization process elevates the stability of ADPN, which is according to the calculated thermodynamic parameters. Based on the calculated electrophilicity index (ω) values for monomer and dimer structure, dimer has a lower electron affinity in comparison to monomer. Actually, the charge transfer between ADPN molecules can be a reason for decreasing the electron affinity.

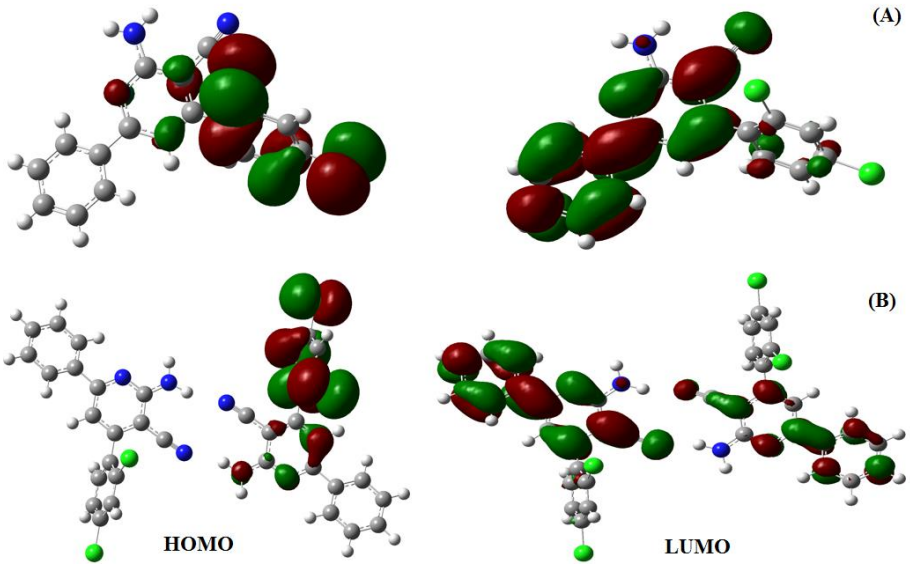

FIGURE 5 The HOMO and LUMO diagrams of ADPN (A) and its dimer (B) at BP86/6-31+G(d) level of theory

TABLE 4 The calculated quantum reactivity indices (eV) of ADPN and its dimer at **BP86/6-31+G(d) level of theory**

	E_L	E_H	ΔE_{L-H}	μ	ω
Monomer	-3.00	-5.78	2.78	-4.39	3.46
Dimer	-2.92	-5.48	2.56	-4.20	3.44

Topological and NCI analysis

To investigate the nature of the interaction between the ADPN molecules in dimer structure, we obtained topological parameters of the H-bonds by applying QTAIM analysis (Table 5). This method calculates the topological parameters at the bond critical points (BCPs). The value of electron density (ρ) at the BCP shows the strength of a given bond. Laplacian (L(r)) represents the curvature of the electron density in a three-dimensional space at the BCP of the atomic interaction. Generally, a negative value of Laplacian shows covalent interactions, while a positive Laplacian confirms the electrostatic interactions. If the ratio of the kinetic energy density (G) and potential energy density (V) (-G/V) is less than 0.5, the interaction is covalent. When the ratio is between 0.5 and 1, the interaction is partly covalent. If the −G/V ratio is greater than 1, the interactions are non-covalent. Therefore, by applying the ratio of −G/V, we can determine the nature of the interactions.

According to Table 5, the calculated ρ of the N3–H5 bond is higher than N8···H28 interaction. In other words, internal interactions are stronger than those of external. The calculated negative values of Laplacian for N3–H5 and N26–H28 bonds reveals a covalent character for these bonds. Moreover, the calculated −G/V ratios for N8···H28 and N3–H5 interactions are greater than 1.0, confirming H-bond formation between ADPN molecules

TABLE 5 The calculated topological parameters at the BCP of the ADPN dimer at **BP86/6-31+G(d) level of theory**

Bonds	ρ	L(r)	-G/V
N8···H28	0.0231	0.0744	1.05
N31···H5	0.0232	0.0746	1.05
N26–H28	0.3092	-0.1537	0.8214
N3–H5	0.3092	-0.1536	0.8293

By employing NCI analysis, it is possible to determine the nature of the interactions based on electron density and the sign of the second derivative in the perpendicular direction of the bond (λ_2). The NCI analysis provides a 2D plot of the reduced density gradient, RDG, in which the sign of λ_2 shows the nature of the interaction.

The $-\lambda_2$ confirms a bonding interaction, such as hydrogen bonds, whereas $+\lambda_2$ shows nonbonding interactions and van der Waals (vdW) interactions can be determined by negligible values of λ2.

According to Figure 6-A, the red, green, and blue ovals indicate repulsion interactions, vdW, and H-bond, respectively. The -λ2 (Figure 6-A), confirms H-bond formation between ADPN molecules. Moreover, a 3D-NCI plots were applied, which is also represented in Figure 6-B. In this plot, the blue, red, and green isosurfaces reveal H-bond, repulsive, and vdW interactions, respectively

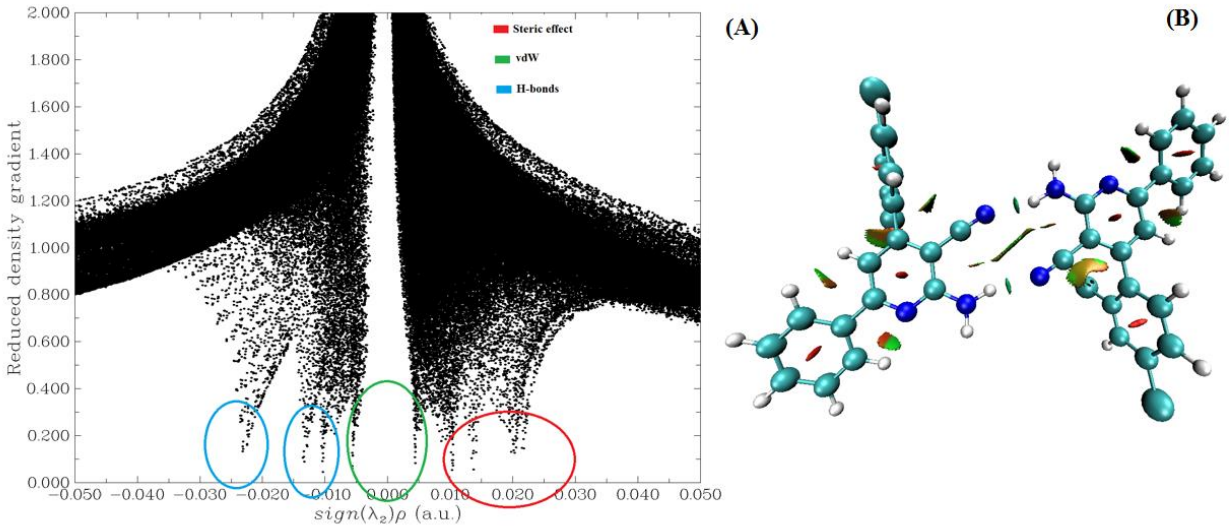

FIGURE 6 The 2D- (A) and 3D-NCI (B) plots of the ADPN dimer

According to Figure 6-B, the blue isosurfaces between CN and NH groups confirm H-bond interactions between ADPN molecules. And green isosurfaces between N atoms of the ring and CH groups reveal a considerable vdW interaction inside the ADPN molecules. NCI analysis reveals that H-bond formation between ADPN molecules is one of the important factors on the stability of dimer structure.

Conclusion

In summary, we prepared single crystal of 2-amino-4-(2,4-dichlorophenyl)-6-phenylnicotinonitrile (ADPN) and characterized it by X-ray single crystal diffraction. Quantum chemistry calculations were applied by using different functionals to investigate the structural and chemical properties of ADPN and its dimer. The calculated structural parameters are in good agreement with experimental data and the obtained dispersion parameters confirmed that dispersion forces have a considerable role in the stability of ADPN crystal. Based on the obtained results from DFT calculations, the nature of the interactions was determined, which can provide remarkable information about the structural features of the reported compound. Moreover, NCI analysis revealed that H-bond formation between ADPN is a driving force for the dimerization process and the main origin of this interaction is donor-acceptor interaction between molecular orbitals.

Acknowledgments

The authors greatly appreciate the University of Zanjan, Iran, for its support

Orcid:

Ali Ramazani: https://orcid.org/0000-0003-3072-7924

Hamideh Ahankar: https://orcid.org/0000-0002-2717-8920

References

[1] A. Sutherland, T. Gallagher, C.G. Sharples, S. Wonnacott, *J. Org. Chem.*, **2003**, *68*, 2475-2478.

[2] N.D. Cosford, L. Tehrani, J. Roppe, E. Schweiger, N.D. Smith, J. Anderson, L. Bristow, J. Brodkin, X. Jiang, I. McDonald, *J. Med. Chem.*, **2003**, *46*, 204-206.

[3] I.J. Enyedy, S. Sakamuri, W.A. Zaman, K.M. Johnson, S. Wang, *Bioorg. Med. Chem. lett.*, **2003**, *13*, 513-517.

[4] F.W. Lichtenthaler, *Acc. Chem. Res.*, **2002**, *35*, 728-737.

[5] V.P. Litvinov, *Russ. Chem. Rev.*, **2003**, *72*, 69-85.
[6] H. Aghahosseini, A. Ramazani, *Eurasian Chem. Commun.*, **2020**, *2*, 410-419.
[7] S. Sajjadifar, M.A. Zolfigol, G. Chehardoli, *Eurasian Chem. Commun.*, **2020**, *2*, 812-818.
[8] F. Mostaghni, F. Taat, *Eurasian Chem. Commun.*, **2020**, *2*, 427-432.
[9] M. Rohaniyan, A. Davoodnia, A. Khojastehnezhad, S.A. Beyramabadi, *Eurasian Chem. Commun.*, **2020**, *2*, 329-339.
[10] S.S. Mansoor, K. Aswin, K. Logaiya, P.N. Sudhan, S. Malik, *Res. Chem. Intermed.*, **2014**, *40*, 871-885.
[11] H.C. Shah, V.H. Shah, N.D. Desai, *Arkivoc*, **2009**, *2*, 76-87.
[12] K. Niknam, R. Rashidian, A. Jamali, *Sci. Iran.*, **2013**, *20*, 1863-1870.
[13] H. Karimi, *Iran. J. Chem. Chem. Eng. (IJCCE)*, **2017**, *36*, 11-19.
[14] Z. Hosseinzadeh, A. Ramazani, N. Razzaghi-Asl, K. Slepokura, T. Lis, *Turk. J. Chem.*, **2019**, *43*, 464-474.
[15] Z. Hosseinzadeh, N. Razzaghi-Asl, A. Ramazani, H. Aghahosseini, A. Ramazani, *Turk. J. Chem.*, **2020**, *44*, 194-213.
[16] A. Ramazani, M. Sheikhi, H. Ahankar, M. Rouhani, S.W. Joo, K. Ślepokura, T. Lis, *J. Chem. Crystallogr.*, **2017**, *47*, 198-207.
[17] A. Ramazani, H. Ahankar, K. Ślepokura, T. Lis, P.A. Asiabi, M. Sheikhi, F. Gouranlou, H. Yahyaei, *J. Chem. Crystallogr.*, **2020**, *50*, 99-113.
[18] A. Ramazani, M. Sheikhi, Y. Hanifehpour, P. Asiabi, S. Joo, *J. Struct. Chem.*, **2018**, *59*, 529-540.
[19] H.-B. Chen, Y. Zhao, Y. Liao, *RSC Adv.*, **2015**, *5*, 37737-37741.
[20] T. Risthaus, S. Grimme, *J. Chem. Theory Comput.*, **2013**, *9*, 1580-1591.
[21] A.E. Reed, L.A. Curtiss, F. Weinhold, *Chem. Rev.*, **1988**, *88*, 899-926.
[22] M. Frisch, G. Trucks, H. Schlegel, G. Scuseria, M. Robb, J. Cheeseman, G. Scalmani, V. Barone, B. Mennucci, G. Petersson, *Wallingford, CT*, **2009**, *32*, 5648-5652.
[23] R. Bader, *Atoms in Molecules: A Quantum Theory*, Oxford University, New York., **1990**.
[24] R. Chaudret, B. De Courcy, J. Contreras-Garcia, E. Gloaguen, A. Zehnacker-Rentien, M. Mons, J.-P. Piquemal, *Phys. Chem. Chem. Phys*, **2014**, *16*, 9876-9891.
[25] T. Lu, F. Chen, *J. Comput. Chem.*, **2012**, *33*, 580-592.
[26] *CrysAlisCCD and CrysAlisRED in KM4-CCD software. Oxford Diffraction Ltd.: Abingdon, England* **2010**
[27] G.M. Sheldrick, *Acta Crystallogr. Sect. A: Found. Crystallogr.*, **2015**, *71*, 3-8.
[28] G.M. Sheldrick, *Acta Crystallogr., Sect. C: Struct. Chem.*, **2015**, *71*, 3-8.
[29] K. Brandenburg, DIAMOND Version 3.2k. Crystal Impact GbR: Bonn, Germany, **2014**
[30] J. Emsley, *Chem. Soc. Rev.*, **1980**, 9, 91-124.

How to cite this article: Zahra Hosseinzadeh*, Mohammad Khavani Sariani, Ali Ramazani*, Hamideh Ahankar, Vasyl Kinzhybalo. Single crystal X-Ray structure and DFT-D3 studies on 2-amino-4-(2,4-dichlorophenyl)-6-phenylnicotinonitrile. *Eurasian Chemical Communications*, 2021, 3(1), 35-44. **Link:** http://www.echemcom.com/article_120553.html